

Chiral nuclear dynamics with three-body forces

J. W. Holt, N. Kaiser and W. Weise
Technische Universität München, Germany

November 28, 2011

Abstract

We review recent progress in implementing high-precision chiral two- and three-body forces in nuclear many-body systems beyond light nuclei. We begin with applications to finite nuclei, which we study through the nuclear shell model and self-consistent mean field theory. We then turn our attention to infinite nuclear matter treated within the framework of Landau's theory of normal Fermi liquids.

1 Introduction

In recent years, the application of chiral effective field theory methods to low-energy nuclear dynamics has resulted in the development of high-precision two- and many-body forces consistent with the symmetry constraints imposed by the fundamental theory of strong interactions, quantum chromodynamics. For recent reviews on this subject, see refs. [1, 2]. Although such interactions have been highly successful in *ab initio* calculations of light-nuclei scattering observables, binding energies and spectra [3, 4, 5], there remains much work to be done to implement three-nucleon forces in studies of medium-mass and heavy nuclei. In this contribution we discuss our recent work to understand the properties of finite nuclei and infinite nuclear matter from many-body perturbation theory employing realistic N³LO chiral two-nucleon forces supplemented with the leading-order N²LO three-body force. For this purpose it is convenient to employ as well low-momentum nucleon-nucleon (NN) interactions [6, 7], which exhibit favorable convergence properties in perturbative calculations [8].

2 In-medium effective nucleon-nucleon interactions

To facilitate the implementation of three-body forces in nuclear many-body calculations, it is useful to construct medium-dependent NN interactions that reflect the most important physical features of the underlying three-nucleon force. Here we focus on a background medium of isospin-symmetric nuclear matter and compute the density-dependent NN interaction to one-loop order from the N²LO chiral three-nucleon interaction. In fact, the effective interaction in nuclear matter with isospin asymmetries up to $\delta_{np} = (\rho_n - \rho_p)/\rho \simeq 0.2$ is already well-approximated by the effective interaction for $\delta_{np} = 0$ [9]. For detailed discussions regarding the in-medium interaction in pure neutron matter, we refer the reader to refs. [9, 10].

The leading-order chiral three-nucleon force includes three separate components of varying range. The two-pion exchange contribution $V_{3N}^{(2\pi)}$ consists of terms proportional to the low-energy constants $c_{1,3,4}$, which arise already in the two-nucleon interaction and can therefore be constrained by fits to

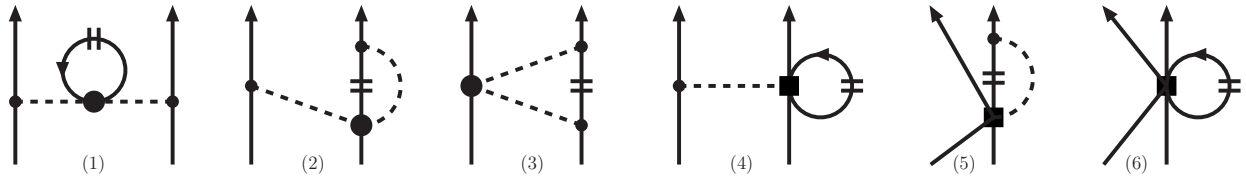


Figure 1: In-medium NN interaction generated by the three different components of the chiral three-nucleon force. The short double-line symbolizes the filled Fermi sea of nucleons, and reflected diagrams are not shown.

NN scattering phase shifts. The one-pion exchange component $V_{3N}^{(1\pi)}$ is proportional to the low-energy constant c_D , while the short-range contact contribution $V_{3N}^{(ct)}$ introduces the low-energy constant c_E . Both c_D and c_E are commonly fit to the properties of $A = 3, 4$ systems. In the present work we use two different parameterizations of the low-energy constants c_E, c_D and $c_{1,3,4}$:

$$c_E = -0.205, \quad c_D = -0.20, \quad c_1 = -0.81 \text{ GeV}^{-1}, \quad c_3 = -3.2 \text{ GeV}^{-1}, \quad c_4 = 5.4 \text{ GeV}^{-1}, \quad (1)$$

$$c_E = -0.625, \quad c_D = -2.06, \quad c_1 = -0.76 \text{ GeV}^{-1}, \quad c_3 = -4.78 \text{ GeV}^{-1}, \quad c_4 = 3.96 \text{ GeV}^{-1}, \quad (2)$$

which are consistent with the Idaho N³LO chiral NN interaction [11] and the low-momentum NN interaction $V_{\text{low-}k}$ evolved to a decimation scale of $\Lambda = 2.1 \text{ fm}^{-1}$ [8], respectively.

At one-loop order there are six distinct diagrams, shown in Fig. 1, contributing to the in-medium NN interaction V_{NN}^{med} . The double-line symbolizes summation over the filled Fermi sea of nucleons, or equivalently, the medium insertion $-2\pi\delta(k_0)\theta(k_f - |\vec{k}|)$ in the in-medium nucleon propagator. For a background medium at rest, the in-medium scattering amplitude for two nucleons in their center of mass frame, $N_1(\vec{p}) + N_2(-\vec{p}) \rightarrow N_1(\vec{p} + \vec{q}) + N_2(-\vec{p} - \vec{q})$, has the same general form as that given in free-space NN scattering. For a background medium boosted with respect to the center of mass frame, the effective interaction will in general depend also on the boost momentum.

In Fig. 2 we plot the 1S_0 and 3S_1 diagonal partial-wave matrix elements of the low-momentum NN potential $V_{\text{low-}k}$ and the modifications resulting from the six components of V_{NN}^{med} evaluated at nuclear matter saturation density ($\rho_0 = 0.16 \text{ fm}^{-3}$) with low-energy constants given in eq. (2). In general, the three contributions from $V_{3N}^{(2\pi)}$ can be a significant fraction of the free-space matrix elements of $V_{\text{low-}k}$ and are considerably stronger than those arising from the one-pion exchange and contact three-nucleon forces. The pion self-energy correction (diagram (1) in Fig. 1) gives rise to an enhancement of the bare 1π -exchange, which can be interpreted in terms of a reduced pion decay constant, $f_{\pi,s}^{*2} = f_\pi^2 + 2c_3\rho$. In contrast, the vertex correction (diagram (2) in Fig. 1) from $V_{3N}^{(2\pi)}$ reduces one-pion exchange, an effect that can be approximated by introducing a reduced nucleon axial-vector constant g_A^* . Taken together, these two terms largely cancel in all partial waves, which leaves the Pauli-blocked two-pion exchange process (diagram (3) in Fig. 1) as a dominant contribution. The contributions from the one-pion exchange three-body force $V_{3N}^{(1\pi)}$ are quite small. Since c_D is negative, the vertex correction (diagram (4) in Fig. 1) reduces the bare 1π -exchange, but only by about 16% at normal nuclear matter density. The pion-loop correction to the NN contact interaction (diagram (5) in Fig. 1) acts only in the two relative S -waves as well as the $S - D$ mixing matrix element. In relative S -waves, it reduces the repulsive contribution from the pure contact term (diagram (6) in Fig. 1) by about one-half. In the right plot of Fig. 2 we sum all six contributions, which together give rise to significant additional repulsion that increases with the density and which provides a mechanism for nuclear matter saturation when employing low-momentum potentials [8].

The resulting in-medium effective interaction has been employed already in shell model studies of finite nuclei, where it was found to play a key role in enhancing the β -decay lifetime of ^{14}C [12] toward

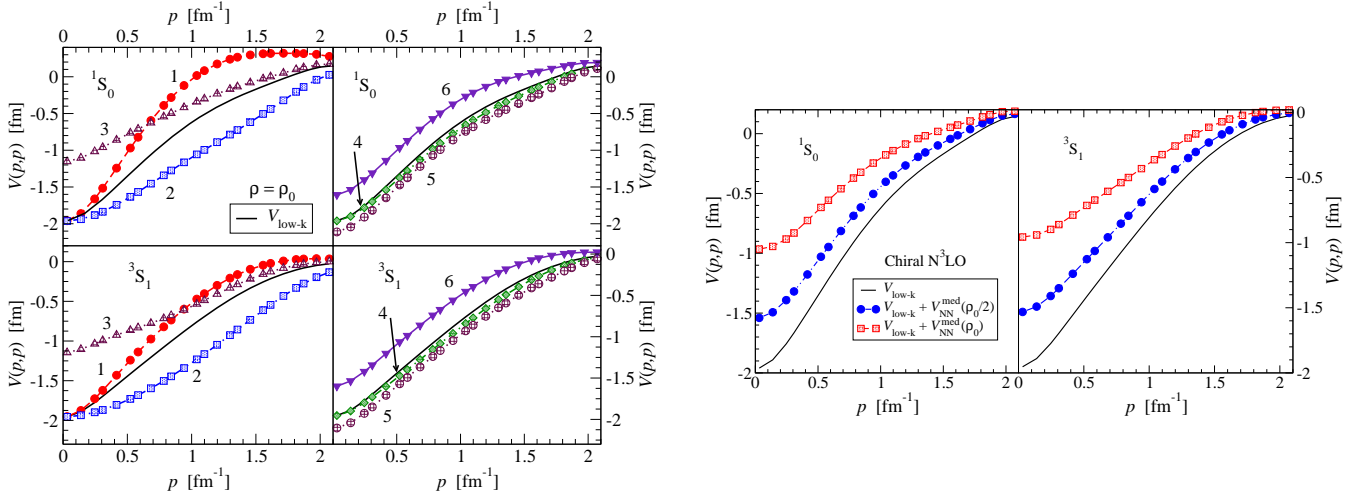


Figure 2: Left figure: contributions to the S -wave effective interaction in symmetric nuclear matter (at saturation density, $\rho_0 = 0.16 \text{ fm}^{-3}$) resulting from the six diagrams shown in Fig. 1. The solid black line shows the matrix elements of the free-space NN potential $V_{\text{low-k}}$, and the labels 1–6 denote the contributions from the corresponding diagrams in Fig. 1. Right figure: contributions from all components of the in-medium NN interaction to the $L = 0$ partial waves at $\rho = \rho_0, \rho_0/2$.

its known archaeologically-long value of 5730 years. An alternative approach for finite nuclei calculations is to evaluate the three-nucleon force in a shell model basis and subsequently sum over the filled orbitals in the closed nuclear core. Such a method has been used to explore the effects of three-nucleon forces in neutron-rich oxygen and calcium isotopes [13].

3 Microscopic energy density functionals

To study the binding energies and charge radii of nuclei across the periodic chart, the most successful theoretical framework has been self-consistent mean field theory based on phenomenological nuclear energy density functionals [14]. A microscopic foundation for such functionals is provided within the framework of many-body perturbation theory by the density matrix expansion of Negele and Vautherin [15], in which the highly nonlocal expression for the energy is expanded in terms of local densities and currents (and their gradients) resulting in a generalized Skyrme functional with density-dependent couplings.

Recently Gebremariam, Duguet and Bogner [16] have developed an improved density matrix expansion that gives rise to a much improved description of the spin density matrix. The form of the density matrix they find (neglecting isovector terms) can be expanded in relative and center-of-mass coordinates, \vec{a} and \vec{r} , as follows:

$$\begin{aligned} \sum_{\alpha} \Psi_{\alpha}(\vec{r} - \vec{a}/2) \Psi_{\alpha}^{\dagger}(\vec{r} + \vec{a}/2) &= \frac{3\rho}{ak_f} j_1(ak_f) - \frac{a}{2k_f} j_1(ak_f) \left[\tau - \frac{3}{5} \rho k_f^2 - \frac{1}{4} \vec{\nabla}^2 \rho \right] \\ &+ \frac{3i}{2ak_f} j_1(ak_f) \vec{\sigma} \cdot (\vec{a} \times \vec{J}) + \dots, \end{aligned} \quad (3)$$

where the spherical Bessel function $j_1(x) = (\sin x - x \cos x)/x^2$. The quantities appearing on the right hand side of eq. (3) are the (local) nucleon density $\rho(\vec{r}) = 2k_f^3(\vec{r})/3\pi^2 = \sum_{\alpha} \Psi_{\alpha}^{\dagger}(\vec{r}) \Psi_{\alpha}(\vec{r})$, the (local) kinetic energy density $\tau(\vec{r}) = \sum_{\alpha} \vec{\nabla} \Psi_{\alpha}^{\dagger}(\vec{r}) \cdot \vec{\nabla} \Psi_{\alpha}(\vec{r})$ and the (local) spin-orbit density $\vec{J}(\vec{r}) = i \sum_{\alpha} \vec{\Psi}_{\alpha}^{\dagger}(\vec{r}) \vec{\sigma} \times \vec{\nabla} \Psi_{\alpha}(\vec{r})$.

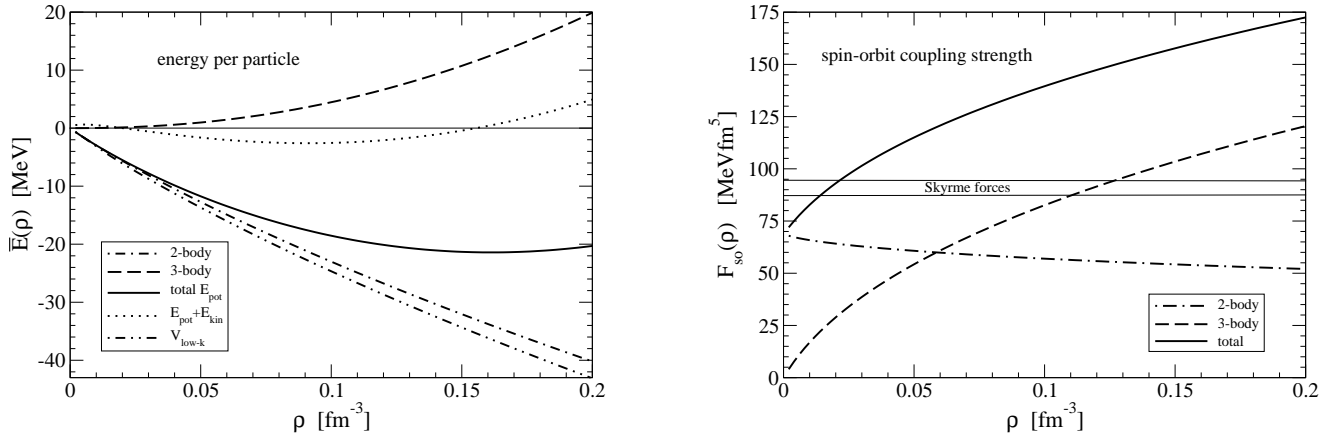


Figure 3: Contributions to the energy per particle $\bar{E}(\rho)$ of isospin-symmetric nuclear matter and to the spin-orbit strength parameter F_{so} as a function of the nuclear density ρ .

The energy density functional resulting from this improved density matrix expansion has been calculated to three-loop order including 1π -exchange, iterated 1π -exchange and irreducible 2π -exchange with intermediate Δ -isobars in ref. [17] and with a microscopic $N^2\text{LO}$ nucleon-nucleon potential in ref. [18]. In our work [19], we have employed a microscopic $N^3\text{LO}$ chiral NN potential supplemented with the $N^2\text{LO}$ chiral three-nucleon force. The two-body interaction is comprised of long-range one- and two-pion exchange contributions together with a set of contact terms contributing up to fourth power in momenta. The potential, referred to as the $N^3\text{LOW}$ chiral NN interaction [20], has a sharp momentum-space cutoff $\Lambda = 2.1 \text{ fm}^{-1}$ corresponding to the scale at which low-momentum interactions become universal and strongly perturbative. The low-energy constants c_E, c_D and $c_{1,3,4}$ of the leading-order chiral three-nucleon interaction are those of eq. (2).

Up to second order in spatial gradients, the energy density functional relevant for $N = Z$ even-even nuclei reads:

$$\mathcal{E}[\rho, \tau, \vec{J}] = \rho \bar{E}(\rho) + \left[\tau - \frac{3}{5} \rho k_f^2 \right] \left[\frac{1}{2M} - \frac{k_f^2}{4M^3} + F_\tau(\rho) \right] + (\vec{\nabla}\rho)^2 F_\nabla(\rho) + \vec{\nabla}\rho \cdot \vec{J} F_{so}(\rho) + \vec{J}^2 F_J(\rho). \quad (4)$$

Due to the nonlocalities present in the chiral contact interactions, it is convenient to compute the density-dependent strength functions $\bar{E}(\rho)$, $F_\tau(\rho)$, $F_d(\rho)$, $F_{so}(\rho)$ and $F_J(\rho)$ separately for the finite-range pion-exchange and the zero-range contact components in the chiral $N^3\text{LO}$ NN interaction. The leading-order three-nucleon force is computed under the assumption that the relevant product of density-matrices can be represented in momentum space in a factorized form: $\Gamma(\vec{p}_1, \vec{q}_1) \Gamma(\vec{p}_2, \vec{q}_2) \Gamma(\vec{p}_3, -\vec{q}_1 - \vec{q}_2)$.

In Figs. 3–5 we plot the density dependence of the five strength functions $\bar{E}(\rho)$, $F_\tau(\rho)$, $F_d(\rho)$, $F_{so}(\rho)$ and $F_J(\rho)$. At first order in perturbation theory, low-momentum interactions are typically underbound after including the leading-order chiral three-nucleon force [8], and this is reflected in the left plot of Fig. 3, where it is seen that both the saturation density and binding energy are too small. In the right plot of Fig. 3 we show the spin-orbit strength, which receives a very large positive contribution from the $N^2\text{LO}$ chiral three-body force that increases the strength at $\rho = \rho_0/2$ beyond values typical of Skyrme functionals. The strength function $F_\tau(\rho)$ (shown in the left plot of Fig. 4) is related to the effective nucleon mass M^* , shown in the right plot of Fig. 4. At saturation density, the effective nucleon mass is $M^* \simeq 0.7 M_N$, within the range of values used in phenomenological functionals. Finally, we consider $F_\nabla(\rho)$ and $F_J(\rho)$ shown in Fig. 5. The former encodes the energy due to density gradients at the Fermi surface, and at half nuclear matter saturation density it achieves values slightly below those extracted from Skyrme functionals. The strong variation at low densities of $F_J(\rho)$ originates from the dominant 1π -exchange contribution [17]. The resulting microscopic energy density functional is an encouraging

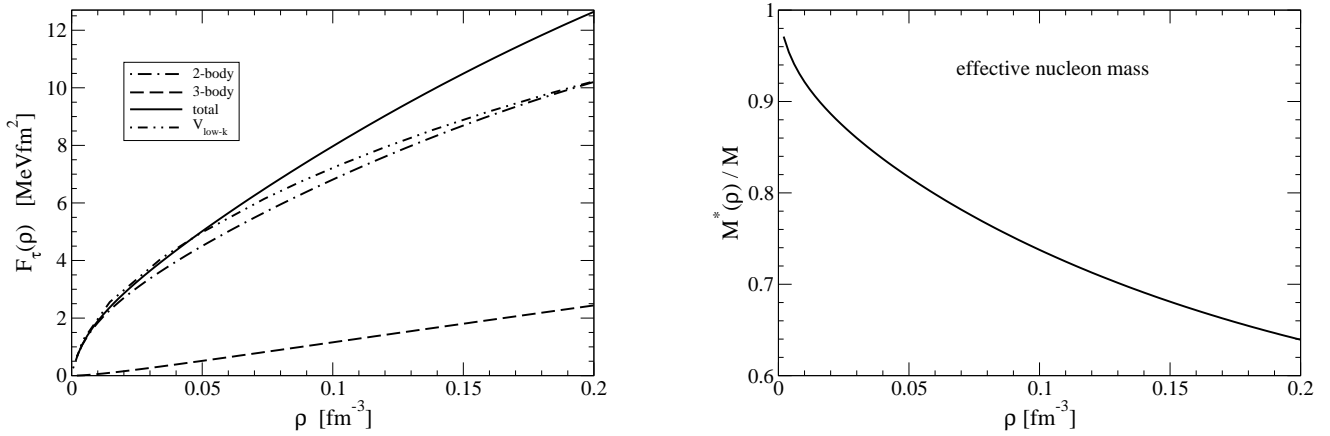


Figure 4: Contributions to the strength parameter F_τ and effective mass M^* as a function of the nuclear density ρ .

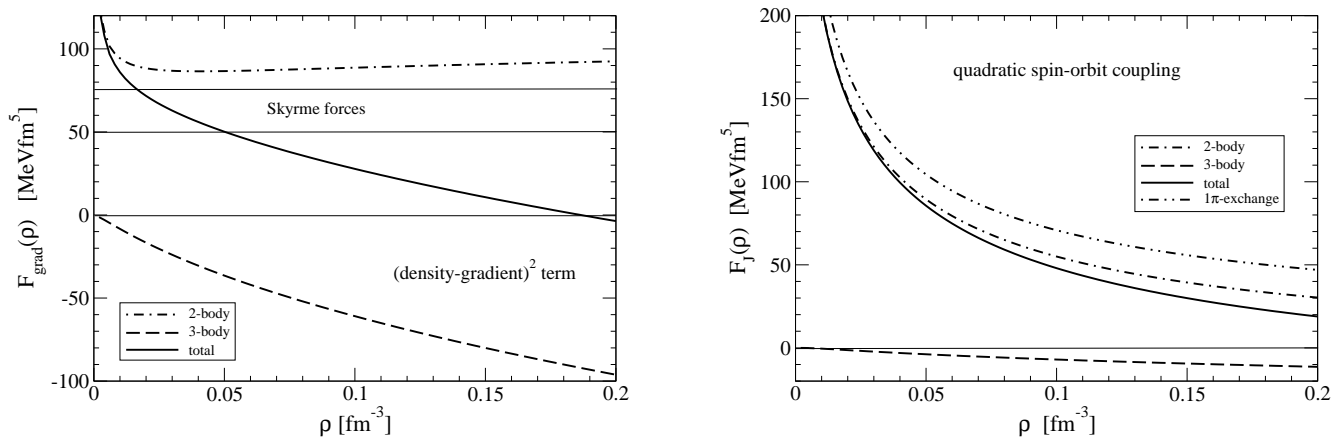


Figure 5: Contributions to the strength parameters F_∇ and F_J as a function of the nuclear density ρ .

start and leaves room for second-order perturbative contributions, which are expected to improve in particular both the energy per particle $\bar{E}(\rho)$ and the spin-orbit strength F_{so} [19].

4 Quasiparticle interaction in nuclear matter

Landau's theory of normal Fermi liquids [21] can be employed to study the bulk equilibrium and transport properties of strongly-interacting normal Fermi systems at low temperatures. The theory describes the low-energy excitations above the interacting ground state in terms of quasiparticles, which retain certain features of noninteracting particles and in a sense are weakly interacting. The quasiparticle interaction encodes bulk properties of the medium and dynamical properties of the quasiparticles themselves. It can be computed in many-body perturbation theory by functionally differentiating the ground-state energy twice with respect to the quasiparticle distribution function and has the form

$$\mathcal{F}(\vec{p}_1, \vec{p}_2) = \frac{1}{N_0} \sum_{L=0}^{\infty} [F_L + F'_L \vec{\tau}_1 \cdot \vec{\tau}_2 + (G_L + G'_L \vec{\tau}_1 \cdot \vec{\tau}_2) \vec{\sigma}_1 \cdot \vec{\sigma}_2] P_L(\cos \theta), \quad (5)$$

where we have expanded the angular dependence in Legendre polynomials, factored out the density of states N_0 at the Fermi surface and included only the central components of the quasiparticle interaction.

	F_0	G_0	F'_0	G'_0	F_1	G_1	F'_1	G'_1	M^*/M_N	\mathcal{K} [MeV]	β [MeV]	δg_l
$V_{\text{N}^3\text{LO}}^{2N}$	-1.64	0.35	1.39	1.59	-0.13	0.50	0.58	0.47	0.96	-150	31	0.12
$V_{\text{low-k}}^{2N}$	-1.98	0.58	1.94	2.14	0.38	0.83	0.87	0.80	1.13	-190	32	0.07
$V_{\text{N}^3\text{LO}}^{3N}$	-0.15	0.35	1.36	1.19	-0.22	0.21	0.28	0.24	0.93	200	31	0.09
$V_{\text{low-k}}^{3N}$	1.48	0.22	1.45	1.48	0.08	0.37	0.41	0.39	1.03	530	29	0.05

Table 1: Dimensionless Fermi liquid parameters at nuclear matter saturation density (corresponding to $k_F = 1.33 \text{ fm}^{-1}$) obtained from chiral two- and three-nucleon interactions as described in the text.

Recently, we have employed chiral two- and three-body forces in a systematic study of the quasiparticle interaction in isospin-symmetric nuclear matter [22, 23]. Already a number of observables (see eq. (6) for the relation to Fermi liquid parameters) were well described in the second-order perturbative calculation that included two-nucleon forces only [22]. In particular, the values of the quasiparticle effective mass M^* , the isospin-asymmetry energy β and the spin-isospin response parameter g'_{NN} were found to be $M^*/M_N \simeq 1.0 - 1.1$, $\beta \simeq 31 - 32 \text{ MeV}$ and $g'_{NN} \simeq 0.65 - 0.75$, all within empirical ranges. However, both the compression modulus $\mathcal{K} \simeq -200 \text{ MeV}$ and the anomalous orbital g -factor $\delta g_l \simeq 0.1$ were found to differ appreciably from the empirical values $\mathcal{K} \simeq 200 - 300 \text{ MeV}$ and $\delta g_l \simeq 0.20 - 0.26$ inferred from studies of giant resonances in heavy nuclei.

As a first step toward the consistent inclusion of the N^2LO chiral three-nucleon force, we have computed the first-order perturbative contribution to the $L = 0, 1$ Landau parameters of the quasiparticle interaction. Two sets of low-energy constants, given in eqs. (1)–(2), were employed, which allowed for an estimate of the theoretical uncertainty at this order in the calculation. The diagrammatic contributions to the quasiparticle interaction are shown in Fig. 1, but since the two quasiparticles lie on the Fermi surface $|\vec{p}_1| = |\vec{p}_2| = k_F$, the kinematics in the present case are different than those considered in Section 2. We show in Table 1 the results from the second-order calculation including two-nucleon forces only (labeled “ $2N$ ”) and the results obtained by including as well the one-loop contributions from the N^2LO chiral three-body force (labeled “ $3N$ ”). We notice that the most visible effect is a dramatic increase in the isotropic spin- and isospin-independent parameter F_0 , which was large and negative (leading to a negative compression modulus \mathcal{K}) when computed with only chiral and low-momentum NN interactions, but which now attains values in reasonable agreement with empirical constraints from giant monopole resonances. In comparison, the contributions to the other Landau parameters from the chiral three-nucleon force considered here are much smaller, and most observables remain in good agreement with their empirical values:

$$\begin{aligned}
\text{Effective mass : } \quad \frac{M^*}{M_N} &= 1 + F_1/3 = && 0.98 \pm 0.05, && [0.7 - 1.0] \\
\text{Anomalous orbital } g\text{-factor: } \quad \delta g_l &= \frac{F'_1 - F_1}{6(1 + F_1/3)} = && 0.07 \pm 0.02, && [0.20 - 0.26] \\
\text{Compression modulus : } \quad \mathcal{K} &= \frac{3k_F^2}{M^*} (1 + F_0) = && (370 \pm 160) \text{ MeV}, && [200 - 300] \text{ MeV} \\
\text{Isospin asymmetry energy : } \quad \beta &= \frac{k_F^2}{6M^*} (1 + F'_0) = && (30 \pm 1) \text{ MeV}, && [30 - 36] \text{ MeV} \\
\text{Spin-isospin response : } \quad g'_{NN} &= \frac{4M_N^2}{g_{\pi N}^2 N_0} G'_0 = && 0.55 \pm 0.03 && [0.6 - 0.7]. \quad (6)
\end{aligned}$$

In these equations, $g_{\pi N} \simeq 13.2$ is the strong πN coupling constant and the values in brackets represent empirical estimates (for further details, see ref. [23]). Moreover, the theoretical uncertainty resulting from different choices of cutoff scale and low-energy constants is reduced with the inclusion of three-nucleon forces. The one observable which remains in disagreement with its empirical value is the

anomalous orbital g -factor δg_l , which lies well below the value $\delta g_l = 0.20 - 0.26$ extracted from a sum-rule analysis of giant dipole resonances. As suggested in ref. [23], this could be remedied if higher-order perturbative calculations reduce even moderately the quasiparticle effective mass M^* . Finally, we notice that all $L = 1$ Landau parameters decrease with the addition of three-nucleon forces, which results in an effective interaction of apparent short range.

5 Conclusion

In this talk we have focused on our recent efforts to incorporate the leading-order chiral three-nucleon force in many-body perturbation theory calculations of dense nuclear systems. This work has set the foundation for future shell model and mean field theory calculations of finite nuclei, and our investigations of infinite isospin-symmetric nuclear matter can be broadened to include pure neutron matter as a first approximation to neutron-star matter. In the future we look forward to employing the recently completed subleading chiral three-nucleon force [24], which will allow for consistent calculations up to order $N^3\text{LO}$ in the chiral expansion.

References

- [1] E. Epelbaum, Prog. Part. Nucl. Phys. **57** (2006) 654.
- [2] D. R. Entem and R. Machleidt, Phys. Rept. **503** (2011) 1.
- [3] E. Epelbaum *et al.*, Phys. Rev. C **66** (2002) 064001.
- [4] H. Witala *et al.*, Phys. Rev. C **73** (2006) 044004.
- [5] P. Navratil *et al.*, Phys. Rev. Lett. **99** (2007) 042501.
- [6] S. K. Bogner, T. T. S. Kuo and A. Schwenk, Phys. Reports **386** (2003) 1.
- [7] S. K. Bogner, R. J. Furnstahl and A. Schwenk, Prog. Part. Nucl. Phys. **65** (2010) 94.
- [8] S. K. Bogner, A. Schwenk, R. J. Furnstahl, and A. Nogga, Nucl. Phys. **A763** (2005) 59.
- [9] J. W. Holt, N. Kaiser and W. Weise Phys. Rev. C **81** (2010) 024002.
- [10] K. Hebeler and A. Schwenk, Phys. Rev. C **82** (2010) 014314.
- [11] D. Gazit, S. Quaglioni, and P. Navratil, Phys. Rev. Lett. **103** (2009) 102502.
- [12] J. W. Holt, N. Kaiser, and W. Weise, Phys. Rev. C **79** (2009) 054331.
- [13] J. D. Holt and A. Schwenk, arXiv:1108.2680 and references therein.
- [14] M. Bender, P. H. Heenen and P. G. Reinhard, Rev. Mod. Phys. **75** (2003) 121.
- [15] J. W. Negele and D. Vautherin, Phys. Rev. **C5** (1972) 1472.
- [16] B. Gebremariam, T. Duguet and S. K. Bogner, Phys. Rev. C **82** (2010) 014305.
- [17] N. Kaiser and W. Weise, Nucl. Phys. **A836** (2010) 256.
- [18] B. Gebremariam, S. K. Bogner and T. Duguet, Nucl. Phys. **A851** (2011) 17.
- [19] J. W. Holt, N. Kaiser, and W. Weise, Eur. Phys. J. A **47** (2011) 128.
- [20] L. Coraggio *et al.*, Phys. Rev. C **75** (2007) 024311.
- [21] L. D. Landau, Sov. Phys. JETP, **3** (1957) 920; **5** (1957) 101; **8** (1959) 70.
- [22] J. W. Holt, N. Kaiser, and W. Weise, Nucl. Phys. **A870-871** (2011) 1.
- [23] J. W. Holt, N. Kaiser, and W. Weise, arXiv:1111.1924.
- [24] V. Bernard, E. Epelbaum, H. Krebs, U.-G. Meissner, Phys. Rev. C **77**, 064004 (2008); arXiv:1108.3816.